DALTON
FULL PAPER

On the electronic structure of $[Pt(4,4'\text{-}X_2\text{-bipy})Cl_2]^{0/-/2-}$: an electrochemical and spectroscopic (UV/Vis, EPR, ENDOR) study

Eric J. L. McInnes,*[a] Robert D. Farley,[b] Christopher C. Rowlands,[b] Alan J. Welch,[c] Lorenzo Rovatti[d] and Lesley J. Yellowlees*[d]

[a] *EPSRC EPR Centre, Department of Chemistry, University of Manchester, Manchester, UK M13 9PL*
[b] *EPSRC ENDOR Service Centre, Department of Chemistry, University of Wales Cardiff, Cardiff, UK CF1 3TB*
[c] *Department of Chemistry, Heriott-Watt University, Riccarton, Edinburgh, UK EH14 4AS*
[d] *Department of Chemistry, University of Edinburgh, Edinburgh, UK EH9 3JJ*

Received 11th June 1999, Accepted 12th October 1999

A series of complexes of general formula $[Pt(4,4'\text{-}X_2\text{-bipy})Cl_2]$ (bipy = 2,2′-bipyridine; X = NH_2, OEt, Me, H, Ph, Cl or CO_2Me) has been prepared and their redox chemistry and UV/Vis spectroscopy examined. The half-wave potential of the first reduction process from cyclic voltammetry varies linearly with the Hammett parameter of X, and also with the MLCT maximum from UV/Vis spectroscopy. The first reduction processes of the complexes with X = OEt, Me, H, Ph, Cl or CO_2Me are reversible and these complexes undergo a second quasi-reversible or irreversible reduction at potentials 580–760 mV more negative. The reduced, 17 e^- species are characterised by EPR spectroscopy and the total platinum contribution (5d and 6p) to the SOMOs is calculated to be only *ca.* 7–12%. The bulk of the unpaired electron density is carried in the bipy ligand π* system and orientation-selective ^1H ENDOR spectra of $[Pt(4,4'\text{-}X_2\text{-bipy})Cl_2]^-$ (X = H or CO_2Me) show that C5 and C5′ carry the greatest spin density among the four ring C(H) positions. The second reduction product of $[Pt(4,4'\text{-}(CO_2Me)_2\text{-bipy})Cl_2]$ is EPR silent indicating spin-pairing of the two reduction electrons in the same orbital in this particular complex.

Derivatisation of the 2,2′-bipyridine (bipy) ligand[1] has been a popular means of controlling electrochemical and photophysical properties of transition metal bipyridyl complexes. Among the many examples studied are $[Ru(4,4'\text{-}X_2\text{-bipy})_3]^{2+}$,[2] $[Ru(4\text{-X-bipy})_3]^{2+}$,[3] $[Mo(4,4'\text{-}X_2\text{-bipy})(CO)_4]$[4] and $[Re(4,4'\text{-}X_2\text{-bipy})(CO)_3Cl]$.[5] By controlled manipulation of the ligand set it is possible to tune physical properties such as redox potentials, absorption maxima and energies and lifetimes of excited states. The 4,4′ derivatives have received most attention, not only because they are synthetically simplest to prepare but also because substitution at these positions offers no steric problems on complexation. Most of these studies have involved complexes with pseudo-octahedral geometry.

However, there are few examples of such studies on square planar complexes, despite the considerable interest in the unusual redox and photophysical properties[6] of α-diimine complexes of d^8 late transition metal ions. One exception has been Cummings and Eisenberg's recent study where they demonstrated tuning of both the energy and lifetime of the excited state of $[Pt(4,4'\text{-}X_2\text{-bipy})(tdt)]$ (X = H, ^{t}Bu, Me, Cl or CO_2Et; tdt = 3,4-toluenedithiolate).[7] The fact that many such species undergo facile one-electron reductions has led to the study of the reduction products, not only with a view to modelling the electronic excited states of the neutral complexes, but also as an opportunity to study transition metal ions in unusual formal oxidation states. Thus, formal platinum(I), rhodium(0) and iridium(0) species have all been generated in this manner.[8–10] The reduced species have been characterised by electron paramagnetic resonance (EPR) and UV/Vis/near IR spectroscopies, and in most cases has led to the conclusion that radical anion ligand species are formed. For example, Fordyce *et al.*[9] formulated the electrochemically generated complexes $[M(bipy)L_2]$ (M = Rh or Ir; L_2 = diene) as $[M^I(bipy^-)L_2]$.

We have previously described the redox chemistry of a series of complexes of general formula $[Pt(bipy)L_2]^{n+}$ (L = Cl^- or CN^-, $n = 0$; L = NH_3, pyridine, PMe_3 or L_2 = ethylenediamine, $n = 2$).[10] We found that such species typically undergo two consecutive one-electron reduction processes separated by 500–700 mV in 0.1 M $[^nBu_4N]BF_4$–DMF (DMF = dimethylformamide) solution. The half-wave potential of the first reduction processes in this series only varied within a range of 160 mV. UV/Vis/near IR and EPR spectroscopic studies of the one-electron reduction products revealed the lowest unoccupied molecular orbital (LUMO) of the parent complex in each case to be predominantly bipy π* based but with significant (*ca.* 10–15% total) admixtures of platinum $5d_{yz}$ and/or $6p_z$ orbitals, depending on the nature of L.[10,11] We now report the synthesis of a series of complexes of general formula $[Pt(4,4'\text{-}X_2\text{-bipy})Cl_2]$ (Fig. 1) and the effect of the substituent X on their electrochemical behaviour. We have recently reported the results for X = NO_2 which exhibited unique redox properties among the series.[12] Where possible we have studied their one- and two-electron reduction products *via* EPR spectroscopy. The EPR spectra of the parent complex $[Pt(bipy)Cl_2]^-$ have already been discussed in detail, and we have also reported a preliminary electron-nuclear double resonance (ENDOR) investigation where we observed hyperfine coupling to both the ^1H and ^{14}N nuclei of the bipy ring.[11] In this work we present a more detailed, orientation-selective ENDOR study of the one-electron reduction products for X = H and CO_2Me which allows us to determine the distribution of the unpaired electron density about the bipy ring system.

Experimental

Syntheses

2,2′-Bipyridine, 4,4′-Me_2-bipy and 4,4′-Ph_2-bipy were commercially available (Aldrich). All other ligands were prepared by literature methods.[1,3] The complexes $[Pt(bipy)Cl_2]$,[13] $[Pt(4,4'\text{-}$

This journal is © The Royal Society of Chemistry 1999

Table 1 Synthesis conditions and analyses of [Pt(4,4′-X_2-bipy)Cl_2]

X	t^a/min	Yield (%)	Analysis (%) C	H	N
NH_2	15	80	25.2[b]	2.7	11.5
			26.6[c]	2.2	12.4
OEt	75	100	32.6	3.3	5.8
			33.0	3.2	5.5
Ph	120	60	46.5	3.0	5.4
			46.0	2.8	4.9
Cl	240	85	27.2	1.8	7.5
			24.5	1.2	5.7
CO_2Me	240	79	31.2	2.3	5.1
			31.2	2.3	5.2

[a] Reflux time. [b] Experimental. [c] Predicted.

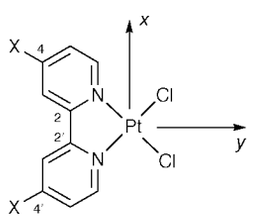

Complex	X
1	NH_2
2	OEt
3	Me
4	Ph
5	H
6	Cl
7	CO_2Me

Fig. 1 Structure and numbering scheme for $[M(4,4'\text{-}X_2\text{-bipy})L_2]^{n+}$.

Me_2-bipy)Cl_2][14] and [Pt(4,4′-Ph_2-bipy)Cl_2][15] were prepared by literature methods. Complexes [Pt(4,4′-X_2-bipy)Cl_2] where X = NH_2, OEt, Cl or CO_2Me were prepared by the following general procedure. A suspension of the appropriate ligand was heated under reflux with stirring in an aqueous solution of $K_2[PtCl_4]$ (1 molar equivalent). The resultant precipitate was filtered off, washed with water, dried *in vacuo* and recrystallised from a saturated hot DMF solution. The complex [Pt(4,4′-$(NH_2)_2$-bipy)Cl_2] decomposed on attempted recrystallisation and was used without further purification. Reflux times, percentage yields and analyses are given in Table 1.

All electrochemical and spectroelectrochemical (UV/Vis/near IR) apparatus was as previously described.[10] *In situ* electrochemical EPR studies used a standard quartz EPR flat cell with a platinum gauze working electrode in the flat section. The Ag–AgCl reference electrode and a wound platinum gauze counter electrode in a fritted PTFE sleeve sit in the solution reservoir at the top of the cell. Redox potentials are quoted *vs.* the ferrocenium–ferrocene couple although experimentally they were measured *vs.* a Ag–AgCl reference electrode immersed in a 0.45 M [^{n}Bu_4N][BF_4]–0.05 M[^{n}Bu_4N]Cl–CH_2Cl_2 solution which was chemically isolated from the solution under study *via* a porous frit. Bulk electrosynthesis experiments were performed on $N_{2(g)}$ purged 0.1 M [^{n}Bu_4N][BF_4]–DMF solutions at 243 K. The UV/Vis spectra were recorded on a Perkin-Elmer λ9 spectrophotometer, X-band EPR spectra on a Bruker ER200D-SCR spectrometer. The ENDOR spectra were recorded on an X-band Bruker ESP300E spectrometer fitted with an ESP360D DICE ENDOR unit. Spectra were recorded for [Pt(bipy)Cl_2]$^-$ and [Pt(4,4′-$(CO_2Me)_2$-bipy)Cl_2]$^-$ in d_7-DMF at 10 K. Spectra were recorded at 5 G intervals between the first two *g* values, and at 10 G intervals between the second and third *g* values, in the frequency range 5–25 MHz.

Results and discussion

Synthesis

The complexes [Pt(4,4′-X_2-bipy)Cl_2] {X = NH_2 **1**, OEt **2**, Me **3**, Ph **4**, H **5**, Cl **6** or CO_2Me **7**} were prepared by heating to reflux a suspension of the appropriate ligand in an aqueous solution of $K_2[PtCl_4]$. The reflux times required to attain a reasonable yield (*ca.* 80%) of the product (varying from 15 min for **1** to 4 h for **7**) depend on the pK_a values of the "free" ligands.

Table 2 Redox potentials of 4,4′-X_2-bipy in 0.1 M [^{n}Bu_4N][BF_4]–DMF at 293 K

X	$E_1{}^a$/V	E_2/C
NH_2	—	—
OEt	−2.88[b]	—
Me	−2.68[c] (0.140)[d]	—
H	−2.60 (0.100)	—
Ph	−2.34 (0.060)	—
Cl	−2.24[b]	—
CO_2Me	−2.03 (0.070)	−2.52 (0.130)

[a] Potentials quoted relative to Fc^+–Fc, measured relative to Ag–AgCl. [b] Irreversible, cathodic peak quoted. [c] $(E_f + E_r)/2$. [d] $E_f - E_r$.

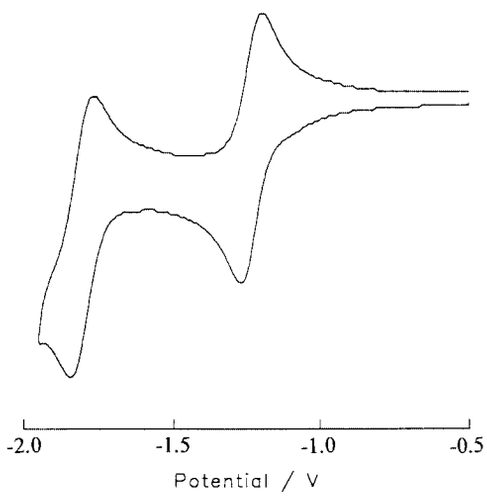

Fig. 2 Cyclic voltammogram of [Pt(4,4′-$(CO_2Me)_2$-bipy)Cl_2] in 0.1 M [^{n}Bu_4N][BF_4]–DMF at 293 K.

Redox chemistry

"Free" ligands. All the ligands studied except X = NH_2, *i.e.* for ligands 4,4′-X_2-bipy with X = OEt, Me, Ph, Cl or CO_2Me, undergo reductive processes as shown by cyclic voltammetry (Table 2); bipy itself (X = H) undergoes a reversible one-electron reduction at −2.60 V *vs.* Fc^+–Fc in 0.1 M [^{n}Bu_4N][BF_4]–DMF solution on our electrode system. The reductions of 4,4′-$(OEt)_2$-bipy and 4,4′-Cl_2-bipy are chemically and electrochemically irreversible at all temperatures (293–243 K) and scan speeds (50–1000 mV s^{-1}) studied. No reduction is observed for 4,4′-$(NH_2)_2$-bipy, presumably because it lies at more negative potentials than the solvent breakdown limit of *ca.* −3.0 V. A second reduction is observed for 4,4′-$(CO_2Me)_2$-bipy at a potential 490 mV more negative than the first.

[Pt(4,4′-X_2-bipy)Cl_2]. Complexes **2**–**7** undergo a fully reversible reduction at potentials ranging from −1.78 to −1.22 V in 0.1 M [^{n}Bu_4N][BF_4]–DMF solution at 293 K (Table 3). A typical cyclic voltammogram is shown in Fig. 2. Coulometric studies at 243 K confirm a one-electron reduction in each case. The reduction of **1** is irreversible at ambient temperatures, showing no anodic peak. However, an associated peak at −0.66 V is observed due to formation of a daughter product. No attempt was made to characterise the latter. At 213 K a return wave for $\mathbf{1}^- \longrightarrow \mathbf{1}$ is observed, yielding an $E_{1/2}$ of −2.08 V.

Thus, the one-electron reduction potential of 4,4′-derivatised 2,2′-bipyridine complexes of Pt can readily be modified by alteration of the substituent. Replacement of NH_2 by NO_2 ($E_{1/2}$ = −0.82 V for X = NO_2)[12] results in a half-wave potential shift of over 1 V. The energy of the LUMO of [Pt(bipy)Cl_2]-type complexes is therefore highly sensitive to the electronic

Table 3 Redox potentials of [Pt(4,4′-X_2-bipy)Cl_2] in 0.1 M [$^nBu_4N$][BF_4]–DMF

Complex	σ_p [a]	E_1 [b]/V	E_2/V	$E_1 - E_2$/V
1	−0.66	−2.08 [c] (0.140) [d]	—	—
2	−0.24	−1.78 (0.070)	−2.41 (0.160)	0.630
3	−0.17	−1.71 (0.070)	−2.47 [e]	0.760
4	−0.01	−1.56 (0.070)	−2.17 (0.110)	0.610
5	0.00	−1.61 (0.070)	−2.34 (0.110)	0.730
6	0.23	−1.38 (0.080)	−2.11 [e]	0.730
7	0.45	−1.22 (0.070)	−1.80 (0.080)	0.580

[a] Hammett parameter of substituent X, ref. 16. [b] Potentials quoted relative to Fc^+–Fc, measured relative to Ag–AgCl. [c] $(E_f + E_r)/2$. [d] $E_f - E_r$. [e] Irreversible, cathodic peak quoted.

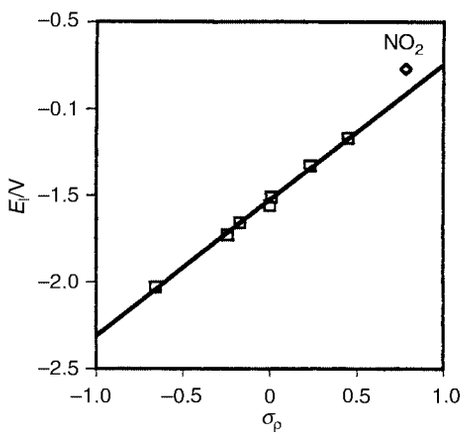

Fig. 3 Plot of E_1 of [Pt(4,4′-X_2-bipy)Cl_2] *vs.* Hammett parameter σ_p of substituent X.

nature of the groups in the 4,4′ position. This stands in contrast to the comparative invariance of the $E_{1/2}$ (*ca.* −1.55 V) of [Pt(bipy)L_2] to the nature of L.[10b]

Complexes **2**–**7** undergo a second reduction process at potentials 580–760 mV more negative than the first. The second reduction is fully reversible for **7** (Fig. 2), quasi-reversible for **2**, **4** and **5** but irreversible for **3** and **6**. In our previous study of [Pt(bipy)L_2]$^{n+}$ we found that the di-reduction products [Pt(bipy)L_2]$^{(n-2)+}$ were unstable on an electrosynthesis timescale at any temperature studied (293–243 K), precluding direct spectroscopic characterisation. However, the electron-withdrawing effect of the CO_2Me groups in complex **7** stabilises the di-reduction product sufficiently to allow bulk electrogeneration of the dianion $\mathbf{7}^{2-}$ at 243 K. Our EPR measurements on $\mathbf{7}^-$ and $\mathbf{7}^{2-}$ indicate that the two added electrons spin-pair in the same orbital (see later) and, hence, we conclude that the $E_1 - E_2$ potential separation is associated with the spin-pairing energy.

The $E_{1/2}$ of the first reduction process of complexes **1**–**7** varies linearly with the Hammett parameter σ_p [16] of the substituent X (Fig. 3). Similar linear correlations have been observed for [Mo(4,4′-X_2-bipy)$(CO)_4$],[4a] [Re(4,4′-X_2-bipy)$(CO)_3$Cl][5] and [Pt(4,4′-X_2-bipy)(tdt)][7] amongst others. Such a correlation is indicative that the acceptor MO has a similar electronic character in each case. Thus, electron withdrawing substituents stabilise the LUMO, while electron-donating substituents destabilise the LUMO of [Pt(4,4′-X_2-bipy)Cl_2] relative to [Pt(bipy)Cl_2]. Hammett parameters are a measure of the inductive influence of a substituent and hence the linear correlation with σ_p implies that the changes in energy of the LUMO are largely being controlled by the σ "push" or "pull" of X, and not π effects. It is interesting that the first $E_{1/2}$ value for [Pt(4,4′-$(NO_2)_2$-bipy)Cl_2][12] does not fit the Hammett curve for complexes **1**–**7** (Fig. 3) which indicates, perhaps unsurprisingly, a significant π effect for this complex.

Table 4 MLCT $\nu_{max}(\varepsilon)$ data for [Pt(4,4′-X_2-bipy)Cl_2] in DMF solution

Complex	MLCT $\tilde{\nu}_{max}/10^3$ cm^{-1}
1	27.6 (0.19) [a]
2	26.2 (0.27)
3	26.0 (0.27)
4	25.0 (0.45)
5	25.7 (0.45)
6	24.8 (0.15)
7	24.1 (0.54)

[a] $\varepsilon/10^4$ M^{-1} cm^{-1}.

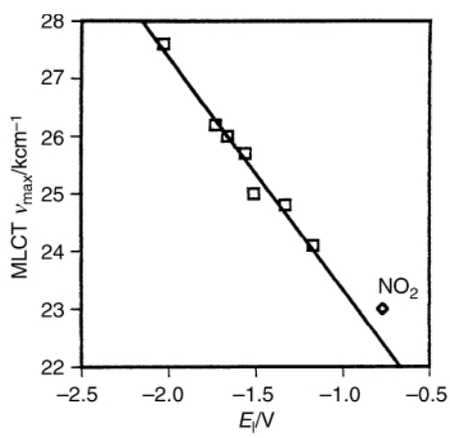

Fig. 4 Plot of E_1 *vs.* MLCT ν_{max} for [Pt(4,4′-X_2-bipy)Cl_2].

UV/Vis Absorption spectroscopy

The complexes [Pt(4,4′-X_2-bipy)Cl_2] all give rise to yellow solutions with UV/Vis spectra similar to that of [Pt(bipy)Cl_2] itself[6a,10] and the spectra can be assigned analogously (Table 4). The lowest energy feature in each case is the metal-to-ligand ($Pt^{II} \rightarrow X_2$bipy π*) charge transfer (MLCT) transition. Other higher energy bands are observed which are combinations of internal π–π* transitions and higher energy MLCT transitions. In agreement with this assignment there is a linear correlation between the first reduction potential, E_1, and the MLCT absorption maximum, ν_{max} (Fig. 4).

EPR Spectroscopy of [Pt(4,4′-X_2-bipy)Cl_2]$^{-/2-}$

The bulk electrochemical one-electron reduction of complexes **2**–**7** to $\mathbf{2}^-$–$\mathbf{7}^-$ in 0.1 M [$^nBu_4N$][BF_4]–DMF solution at 243 K yields EPR active solutions. Complex **1** was not studied due to the irreversibility of its reduction. The room temperature solution EPR spectra of $\mathbf{2}^-$–$\mathbf{7}^-$ are all similar, exhibiting coupling of the unpaired electron with platinum in natural abundance (^{195}Pt, 34%, nuclear spin, $I = 1/2$) with any superhyperfine coupling to the ligand nuclei unresolved. Complexes **2**–**7** can be chemically reduced with $NaBH_4$ to give rise to spectra which are identical to those generated by electrochemical reduction.

On cooling to 77 K rhombic X-band EPR spectra are observed similar to those previously found [10,11] for complex $\mathbf{5}^-$. The spectra can be simulated [17] using the parameters in Table 5. Note that the ^{195}Pt hyperfine splitting about the high-field g_{zz} component (A_{zz}) is not resolved in any of the spectra, and the magnitudes of A_{zz} are estimated to have an uncertainty of $\pm 5 \times 10^{-4}$ cm^{-1}. Typical experimental and simulated spectra are shown in Figs. 5(a) and 6(a), (b).

The similarity of the EPR spectra of complexes $\mathbf{2}^-$–$\mathbf{7}^-$ indicates a common ground state orbital in each case. In our previous study [10,11] of [Pt(bipy)L_2]$^-$ (L = Cl^- or CN^-) we concluded that the ground state orbital was of b_2 symmetry (in C_{2v} point symmetry) where the metal contributions to the singly occupied molecular orbital (SOMO) consisted of small $5d_{yz}$ and $6p_z$ admixtures (in the axis system defined in Fig. 1). Following

Table 5 EPR parameters for $[Pt(4,4'\text{-}X_2\text{-bipy})Cl_2]^-$

Complex	g_{iso} [a]	g_{yy} [b]	g_{xx}	g_{zz}	A_{iso} [c]	A_{yy}	A_{xx}	A_{zz}
2$^-$	2.001	2.028	2.008	1.962	−44	−45(10) [d]	−52(10)	−18(10)
3$^-$	1.999	2.035	2.010	1.946	−51	−55(10)	−70(11)	−18(23)
4$^-$	1.999	2.040	2.009	1.940	−54	−55(9)	−78(10)	−27(23)
5$^-$	1.998	2.038	2.011	1.938	−54	−57(10)	−81(11)	−21(27)
6$^-$	2.000	2.040	2.012	1.941	−51	−54(10)	−79(10)	−25(36)
7$^-$	1.997	2.052	2.009	1.926	−60	−59(10)	−85(10)	−27(27)

[a] Isotropic data and [b] anisotropic data in 0.1 M $[^nBu_4N][BF_4]$–DMF, simulated parameters quoted. [c] $A/10^{-4}$ cm^{-1}. [d] Linewidth used in simulation (10^{-4} cm^{-1}).

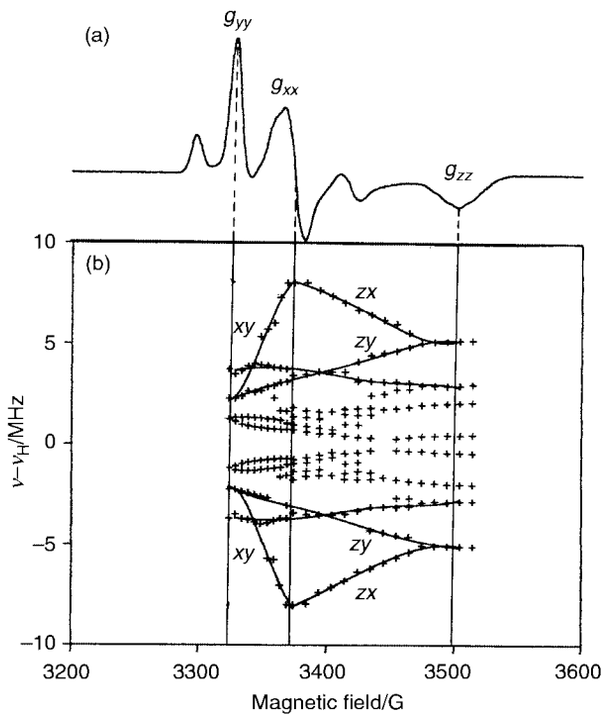

Fig. 5 (a) X-Band EPR spectrum of $[Pt(bipy)Cl_2]^-$ and (b) ^{1}H ENDOR resonances *vs.* magnetic field.

Rieger's methodology[18] we were able to analyse the ^{195}Pt hyperfine matrix in order to calculate the unpaired electron spin densities in the $5d_{yz}$ and $6p_z$ orbitals (a^2 and b^2, respectively), from eqns. (1)–(3) where P_d and P_p are the electron nuclear

$$A_{xx} = A_s - (4/7)P_d a^2 - (2/5)P_p b^2 \quad (1)$$

$$A_{yy} = A_s + (2/7)P_d a^2 - (2/5)P_p b^2 \quad (2)$$

$$A_{zz} = A_s + (2/7)P_d a^2 + (4/5)P_p b^2 \quad (3)$$

dipolar coupling parameters for platinum 5d and 6p electrons, respectively, and A_s is the isotropic Fermi contact term. Using the values $P_d = 549 \times 10^{-4}$ cm^{-1} and $P_p = 402 \times 10^{-4}$ cm^{-1}, calculated assuming a $5d^8$ configuration,[11,18] we can derive values for a^2 and b^2 (Table 6). We justify this treatment and the assignment of the *x*,*y*,*z* axes elsewhere.[11]

In each case the contributions from the metal orbitals to the SOMO consist of almost equally small amounts of $5d_{yz}$ and $6p_z$, although the latter is always slightly larger. The total metal contributions to the SOMOs are in the range 7–12%, thus confirming a predominantly ligand-based orbital in each case. One apparent trend is that the $5d_{yz}$ admixture to the SOMO increases as X becomes a stronger electron-withdrawing group, and this is reflected in the increasing *g* anisotropy (Tables 5 and 6). As the energy of the ligand π* (b_2) orbital is decreased by stronger electron-withdrawing substituents there will be a better energy match with the filled low-lying platinum $5d_{yz}$ (b_2) orbital and, hence, a more efficient metal–ligand orbital overlap. This

Table 6 Platinum $5d_{yz}$ and $6p_z$ admixtures to the SOMO of $[Pt(4,4'\text{-}X_2\text{-bipy})Cl_2]^-$

Complex	$P_d a^2$	$P_p b^2$	a^2	b^2	Total Pt
2$^-$	8.2	23	0.015	0.057	0.07
3$^-$	18	30	0.033	0.075	0.11
4$^-$	27	24	0.049	0.060	0.11
5$^-$	28	30	0.051	0.075	0.13
6$^-$	29	23	0.053	0.057	0.11
7$^-$	30	27	0.055	0.067	0.12

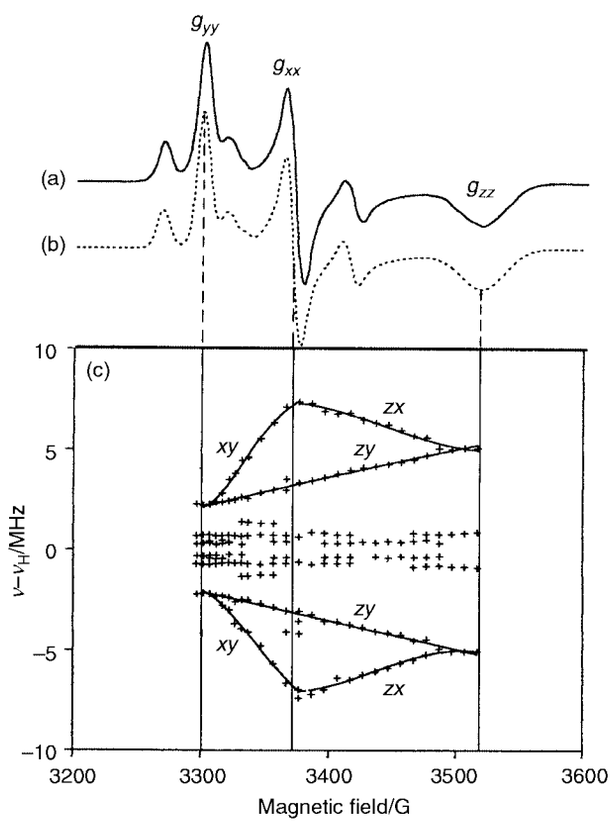

Fig. 6 (a) X-Band EPR spectrum of $[Pt(4,4'\text{-}(CO_2Me)_2\text{-bipy})Cl_2]^-$, (b) simulation using the parameters in Table 5, and (c) ^{1}H ENDOR resonances *vs.* magnetic field.

results in a still predominantly ligand-based π* orbital, but with greater metal 5d character.

On di-reduction of complex **7** to $\mathbf{7}^{2-}$ at −1.45 V and 243 K an EPR signal is obtained at 77 K identical to that of **7**$^-$ but with greatly reduced intensities. This signal is due to residual monoanion **7**$^-$, where $\mathbf{7}^{2-}$ is EPR silent. Thus, the second added electron, corresponding to the second reduction process in the cyclic voltammogram, is spin-pairing with the first added electron in the *same* π* orbital to yield a diamagnetic product. This is consistent with the potential separation of E_1 and E_2 of 580 mV and we conclude that the spin-pairing energy of the two reduction electrons is less than the LUMO − second LUMO

(SLUMO) energy gap. The similar $E_1 - E_2$ separations for complexes **2**–**6** (we do not observe the second reduction for **1**) suggest an analogous MO scheme. Braterman *et al.*[8c,d] have concluded from UV/Vis/near IR spectra of similar species such as $[Pt(bipy)(py)_2]$ (who report the parent complex $[Pt(bipy)(py)_2]^{2+}$ to undergo two reversible reductions at −0.83 and −1.52 V *vs.* Ag–$AgNO_3$ in $[^nBu_4N][BF_4]$–DMF solution) that the first reduction is bipy-localised while the second is metal-localised. We contend that both processes involve the *same* bipy-π*/Pt 5d/6p molecular orbital. A similar set of results has been observed for the redox family $[Rh(bipy)(cod)]^{+/0/-}$ (cod = cycloocta-1,5-diene) where the mono-reduced (uncharged) species is EPR active but the di-reduced (mono-anionic) species is EPR silent.[9] This behaviour stands in contrast to that of $[Pt(4,4'\text{-}(NO_2)_2\text{-bipy})Cl_2]$ which undergoes *four* one-electron reductions, where the $E_1 - E_2$ gap is much smaller at 180 mV, and *both* the first *and* second reduction products are EPR active.[12] Hence for this complex the LUMO − SLUMO gap is smaller than the spin-pairing energy and the two reduction electrons of the dianion enter different molecular orbitals. Thus by judicious choice of the substituent X it is possible not only to fine tune the electron accepting properties of the $[Pt(4,4'\text{-}X_2\text{-bipy})Cl_2]$ system, but also to change the gross nature of the accepting molecular orbitals.

ENDOR Spectroscopy of $[Pt(4,4'\text{-}X_2\text{-bipy})Cl_2]^-$ (X = H or CO_2Me)

The EPR results show that the total metal contribution to the SOMO of $[Pt(4,4'\text{-}X_2\text{-bipy})Cl_2]^-$ is at most 12%. Thus, the bulk of the electron density is carried in the ligand π* system. ENDOR spectroscopy allows us to observe directly the interaction of the unpaired electron with ligand nuclei. Figs. 5(b) and 6(c) illustrate the changes in the ^1H ENDOR spectra of complexes $\mathbf{5}^-$ and $\mathbf{7}^-$ when measured at regular intervals across the EPR spectra. Each vertical slice represents a single ENDOR spectrum. Note that each hyperfine interaction a_H to a ^1H nucleus is manifested as a pair of resonances separated by a_H and centered on ν_H (the resonant frequency for the free proton, 14.902 MHz at 3500 G). Representative ENDOR spectra are shown in Fig. 7 (some spectra for $\mathbf{5}^-$ are also shown in ref. 11).

Since the unpaired electron resides in a π* orbital the ^1H 1s orbitals cannot directly admix to the SOMO. Thus the observed ^1H splittings must arise *via* spin polarisation of the unpaired electron density in the corresponding carbon $2p_z$ orbital. This mechanism is well understood, and the local axes for the ^1H hyperfine matrix are expected to be: (i) co-parallel with the direction of the $2p_z$ orbital of the associated C atom, (ii) co-parallel with the C–H bond, and (iii) perpendicular to (i) and (ii).[19] However, (ii) and (iii) can be skewed if there is significant upe (upe = unpaired electron) density on neighbouring C atoms.[19]

For the system in Fig. 1 this means that all the ^1H positions have a principal axis that is co-parallel with one of the molecular axes: the *z* axis, perpendicular to the plane of the molecule. The *z* axis corresponds to the high-field *g* value in the EPR spectra. Since only a very small range of orientations will contribute to the extremities of a powder EPR spectrum, a single orientation type ENDOR spectrum will be observed at static magnetic fields corresponding to g_{zz}. Thus, the ^1H hyperfine couplings observed at g_{zz} can simply be read from the ENDOR spectra and are principal values. For example, for complex $\mathbf{5}^-$ where there are four magnetically distinct ring ^1H positions (Fig. 1), four clearly resolved pairs of resonances are observed at g_{zz} (Fig. 7a). For $\mathbf{7}^-$ there are three magnetically distinct ring ^1H positions, but only two pairs of resonances are clearly observed at g_{zz} (Fig. 7b). The third coupling must be considerably smaller and obscured by the matrix signal (which arises from the CO_2Me groups and excess of $NaBH_4$ in solution). The

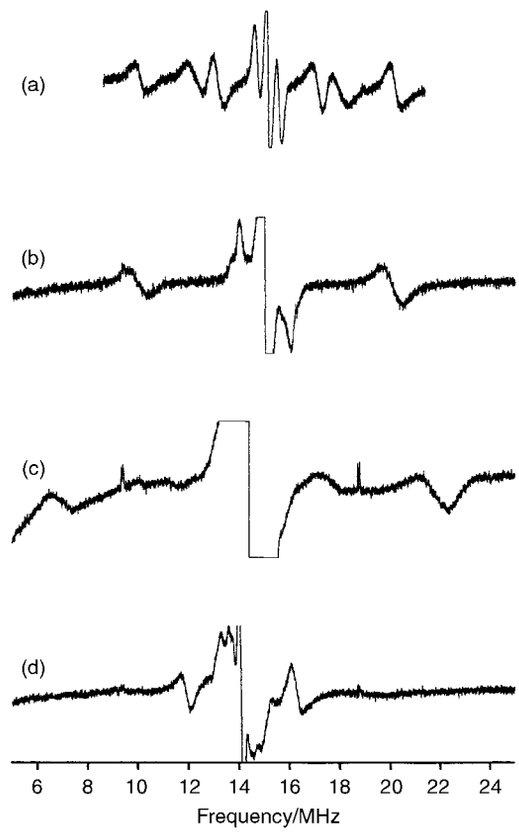

Fig. 7 Representative ^1H ENDOR spectra of (a) $[Pt(bipy)Cl_2]^-$ and (b)–(d) $[Pt(4,4'\text{-}(CO_2Me)_2\text{-bipy})Cl_2]^-$ in d_7-DMF solution at 10 K. Static magnetic fields correspond to (a) g_{zz}, (b) g_{zz}, (c) g_{xx} and (d) g_{yy}.

other two principal axes for each of the ^1H positions must lie within the molecular *xy* plane, and hence will be observed in the ENDOR spectra at static magnetic fields that lie between g_{yy} and g_{xx}.

As the magnetic field is decreased from g_{zz} a wider range of orientations is selected, in the *zx* and *zy* planes, and consequently the ENDOR spectra become more complicated. For example, the outermost pair of resonances at g_{zz} for complex $\mathbf{7}^-$ (*i.e.* the biggest ^1H hyperfine coupling) split into two separate couplings as the field is decreased (Fig. 6c). These correspond to orientations in the *zx* plane and the *zy* plane.[20] One of the pairs of lines moves apart to a maximum separation at *ca.* g_{xx} whilst the other pair decreases in separation to a minimum at *ca.* g_{yy}. These "turning points" correspond to the other principal values for this particular ^1H position. Thus, for this ^1H we can confidently measure the three principal values of the ^1H hyperfine matrix. Furthermore, for the following reasons we can assign these splittings to the C(H)5 and C(H)5′ positions. (a) In EPR studies of the radical anion $bipy^-$ the largest ^1H couplings are observed to C(H)5,5′.[21] (b) Density functional theory (DFT) calculations on $\mathbf{5}^-$ predict the spin densities about the ring to decrease in the order C5,5′ > C2,2′ > N1,1′ > C4,4′ > C3,3′ > C6,6′.[11] Hence, we expect the largest splittings to arise from C(H)5,5′ (C2,2′ are the bridge carbons and have no attached ^1H nuclei); (c) a very similar pattern is observed for $\mathbf{5}^-$ (Fig. 5b). Assuming a similar spin distribution in the two systems,† this rules out the C4,4′ positions which are blocked in $\mathbf{7}^-$. (d) The local axes appear approximately to coincide with the molecular axes, *i.e.* the turning points occur at magnetic fields close to the three *g* values. Only the protons at C5 and 5′ come close to meeting this condition. With a N–Pt–N

† EHMO calculations confirm the LUMO of complex **7** to be similar to that of **5**; C5,5′ are the most significant of the three distinct C(H) positions of **7**, although the CO_2Me groups also contribute significantly to the π* orbital.[22]

bite angle[11] of 80° the C–H bond would make an angle of *ca.* 10° to the molecular *x* axis.

With this assignment it seems likely that the next largest splittings observed in complex $\mathbf{5}^-$ (but not $\mathbf{7}^-$) are from the C(H)4,4′ positions. This is supported by the fact that the maximum splitting is found approximately half-way between g_{xx} and g_{yy}, since the C–H bond at this position makes an angle of *ca.* 50° to the molecular *x* axis.

Positions C3,3′ and C6,6′ are expected to have very small upe densities, and thus small ^{1}H hyperfine couplings. This, together with the ^{1}H matrix signal, contributes to the central region of the ENDOR spectra being very complicated and consequently difficult to interpret.

Thus, the ^{1}H hyperfine matrices for C(H)5,5′ in complexes $\mathbf{5}^-$ and $\mathbf{7}^-$ have the principal values (4.5, 16.1, 10.2 MHz) and (4.4, 14.8, 10.1 MHz), respectively. These would give rise to isotropic values of 10.3 (3.7) and 9.8 MHz (3.5 G), respectively. It is only possible to measure two of the three principal values for C(H)4,4′ in $\mathbf{5}^-$ with confidence, although the third value is likely to be the smallest, giving the principal hyperfine values (<3, 7.8, 5.8 MHz, and an isotropic value <5.5 MHz or <2 G). The McConnell equation[23] allows us to calculate the upe density (ρ_C) in the carbon $2p_z$ orbital contributing to the π system from the value of the isotropic hyperfine coupling (a_H) to the associated α-proton, eqn. (4) where Q_{CH}^H is the coupling constant

$$a_H = Q_{CH}^H \rho_C \qquad (4)$$

for unit population of the carbon 2p orbital (*ca.* 23 G). Substituting the experimental values for a_H gives $\rho_C(5,5') = 0.15$ for $\mathbf{7}^-$, and $\rho_C(5,5') = 0.16$ and $\rho_C(4,4') < 0.09$ for $\mathbf{5}^-$. Thus, the C5 and C5′ atoms in $\mathbf{7}^-$ carry 30% of the unpaired electron density between them, while the C4,4′,5,5′ positions in $\mathbf{5}^-$ account for a total of up to 50% of the unpaired electron density. DFT Calculations predict $\rho_C(5,5') = 0.123$ and $\rho_C(4,4') = 0.051$ for $\mathbf{5}^-$, which constitutes a good agreement between experiment and theory.

Conclusions

Electrochemical and UV/Vis spectroscopic data demonstrate that the LUMO of [Pt(4,4′-X_2-bipy)Cl_2] can be varied over a wide energy range (over 1 eV), and thus derivatisation of the ligand at the 4,4′ positions is a viable method for tuning the physical properties of this class of compound. The EPR and ENDOR data of the one-electron reduced [Pt(4,4′-X_2-bipy)Cl_2]$^-$, while showing minor variations through the series, show that the MO composition of the SOMO does not change significantly. Taking advantage of the orientation selectivity of the ENDOR technique allows us to determine that the C5 and C5′ ring positions contribute more to the redox-active orbital than C4,4′. We might therefore expect that the electronic properties of the system will be more sensitive to substituents in the C5,5′ positions. We are now investigating this effect.

Acknowledgements

We thank Drs. F. E. Mabbs, D. Collison (EPSRC cwEPR Service Centre, University of Manchester) and D. M. Murphy (EPSRC ENDOR Service Centre, University of Wales, Cardiff) for many helpful discussions. We are grateful to the EPSRC for the funding of the national EPR and ENDOR centres, and to the Wolfson (Scotland) Trust for a studentship.

References

1 F. H. Case, *J. Am. Chem. Soc.*, 1946, **68**, 2574; G. Maerker and F. H. Case, *J. Am. Chem. Soc.*, 1958, **80**, 2745; W. H. F. Sasse and C. P. Whittle, *J. Chem. Soc.*, 1961, 1347; C. P. Whittle, *J. Heterocycl. Chem.*, 1977, **14**, 191; K. D. Bos, J. G. Kraaijkamp and J. G. Noltes, *Synth. Commun.*, 1979, **9**, 497; D. Wenkert and R. B. Woodward, *J. Org. Chem.*, 1983, **8**, 283.

2 M. A. Weiner and A. Basu, *Inorg. Chem.*, 1980, **19**, 2797; A. Basu, M. A. Weiner, T. C. Strekas and H. D. Gafney, *Inorg. Chem.*, 1982, **21**, 1085; A. Basu, H. D. Gafney and T. C. Strekas, *Inorg. Chem.*, 1982, **21**, 2231; S. Anderson, E. C. Constable, K. R. Seddon, J. E. Turp, J. E. Baggott and M. J. Pilling, *J. Chem. Soc., Dalton Trans.*, 1985, 2247; R. J. Donohoe, C. D. Tait, M. K. De Armond and D. W. Wertz, *J. Phys. Chem.*, 1986, **90**, 3923, 3927; M. Furue, K. Maruyama, T. Oguni, M. Naiki and M. Kamachi, *Inorg. Chem.*, 1992, **31**, 3792.

3 C. M. Elliot and E. J. Hershenhart, *J. Am. Chem. Soc.*, 1982, **104**, 7519; M. J. Cook, A. P. Lewis, G. S. G. McAuliffe, V. Skerda, A. J. Thomson, J. L. Glasper and D. J. Robbins, *J. Chem. Soc., Perkin Trans. 2*, 1984, 1293, 1303.

4 (*a*) J. A. Connor, C. Overton and N. E. Murr, *J. Organomet. Chem.*, 1984, **277**, 277; (*b*) P. N. W. Baxter and J. A. Connor, *J. Organomet. Chem.*, 1988, **355**, 193.

5 L. A. Worl, R. Deusing, P. Chen, L. D. Ciana and T. J. Meyer, *J. Chem. Soc., Dalton Trans.*, 1991, 849.

6 (*a*) P. M. Gidney, R. D. Gillard and B. T. Heaton, *J. Chem. Soc., Dalton Trans.*, 1973, 132; (*b*) D. L. Webb and L. A. Rossiello, *Inorg. Chem.*, 1971, **10**, 2213; (*c*) V. M. Miskowski and V. H. Holding, *Inorg. Chem.*, 1989, **28**, 1529; (*d*) V. M. Miskowski, V. H. Holding, C.-M. Che and Y. Wang, *Inorg. Chem.*, 1993, **32**, 2518; (*e*) R. Ballardini, M. T. Gandolfi, L. Prodi, M. Ciano, V. Balzani, F. H. Kohnke, H. Shahrini-Zavareh, N. Spencer and J. F. Stoddart, *J. Am. Chem. Soc.*, 1989, **111**, 7072; (*f*) C.-M. Che, K.-T. Wan, L.-Y. He, C.-K. Poon and V. W.-W. Yam, *J. Chem. Soc., Chem. Commun.*, 1989, 943; (*g*) J. Biedermann, M. Walfahrer and G. Gliemann, *J. Lumin.*, 1987, **37**, 323.

7 S. D. Cummings and R. Eisenberg, *J. Am. Chem. Soc.*, 1996, **118**, 1949.

8 (*a*) J. A. Zuleta, M. S. Burbery and R. Eisenberg, *Coord. Chem. Rev.*, 1991, **30**, 4446; (*b*) J. B. Cooper, S. M. Rhodes and D. W. Wertz, *J. Phys. Chem.*, 1991, **95**, 4800; (*c*) P. S. Braterman, J.-I. Song, C. Vogler and W. Kaim, *Inorg. Chem.*, 1992, **31**, 222; (*d*) P. S. Braterman, J.-I. Song, F. W. Wimmer, S. Wimmer, W. Kaim, A. Klein and R. D. Peacock, *Inorg. Chem.*, 1992, **31**, 5084; (*e*) A. Klein and W. Kaim, *Organometallics*, 1995, **14**, 1176; (*f*) S. Hasenzahl, H.-D. Hausen and W. Kaim, *Chem. Eur. J.*, 1995, **1**, 95; (*g*) C. Vogler, B. Schwederski, A. Klein and W. Kaim, *J. Organomet. Chem.*, 1992, **436**, 367; (*h*) G. Minghetti, M. I. Pilo, G. Sanna, R. Seeber, S. Stoccoro and F. Laschi, *J. Organomet. Chem.*, 1993, **452**, 257; (*i*) A. Klein, W. Kaim, E. Waldhör and H.-D. Hausen, *J. Chem. Soc., Perkin Trans. 2*, 1995, 2121; (*j*) F. P. Fanizzi, G. Natile, M. Lanfranchi, A. Tiripocchio, F. Laschi and P. Zanello, *Inorg. Chem.*, 1996, **35**, 3173; (*k*) M. G. Hill, J. A. Bailey, V. M. Miskowski and H. B. Gray, *Inorg. Chem.*, 1996, **35**, 4585.

9 W. A. Fordyce, K. H. Pool and G. A. Crosby, *Inorg. Chem.*, 1982, **21**, 1027.

10 (*a*) S. A. Macgregor, E. J. L. McInnes, R. J. Sorbie and L. J. Yellowlees, *Molecular Electrochemistry of Inorganic, Bioinorganic and Organometallic Compounds*, eds. A. J. L. Pombeiro and J. A. McCleverty, Kluwer, Dordrecht, 1993, p. 503; (*b*) D. Collison, F. E. Mabbs, E. J. L. McInnes, K. J. Taylor, A. J. Welch and L. J. Yellowlees, *J. Chem. Soc., Dalton Trans.*, 1996, 329.

11 E. J. L. McInnes, R. D. Farley, S. A. Macgregor, K. J. Taylor, L. J. Yellowlees and C. C. Rowlands, *J. Chem. Soc., Faraday Trans.*, 1998, 2985.

12 E. J. L. McInnes, A. J. Welch and L. J. Yellowlees, *Chem. Commun.*, 1996, 2393.

13 G. T. Morgan and F. H. Burstall, *J. Chem. Soc.*, 1934, 965.

14 E. Bielli, P. M. Gidney, R. D. Gillard and B. T. Heaton, *J. Chem. Soc., Dalton Trans.*, 1974, 2133.

15 J. A. Zuleta, M. S. Burbery and R. Eisenberg, *Coord. Chem. Rev.*, 1990, **97**, 47.

16 C. Hansch, A. Leo and R. W. Taft, *Chem. Rev.*, 1991, **91**, 165.

17 F. E. Mabbs and D. Collison, *Electron Paramagnetic Resonance of d Transition Metal Compounds*, Elsevier, Amsterdam, 1992, ch. 7.

18 P. H. Rieger, *J. Magn. Reson.*, 1997, **124**, 140.

19 N. M. Atherton, *Principles of Electron Spin Resonance*, Ellis Horwood, Chichester, 1993, ch. 5.6.

20 B. M. Hoffman, J. Martinsen and R. A. Venters, *J. Magn. Reson.*, 1984, **59**, 110.

21 For example, J. Boersma, A. Mackor and J. G. Woltes, *J. Organomet. Chem.*, 1975, **99**, 337.

22 L. J. Yellowlees, unpublished results.

23 N. M. Atherton, *Principles of Electron Spin Resonance*, Ellis Horwood, Chichester, 1993, ch. 3; H. M. McConnell, *J. Chem. Phys.*, 1958, **24**, 764.

Paper 9/04658E